

## Discotic Micellar Nematic and Lamellar Phases under Shear Flow.

J. T. MANG(\*), S. KUMAR(\*) and B. HAMMOUDA(\*\*)

(\*) *Department of Physics and Liquid Crystal Institute, Kent State University  
Kent, OH 44242, USA*

(\*\*) *National Institute of Standards and Technology, Gaithersburg, MD 20899, USA*

(received 19 July 1994; accepted 19 October 1994)

PACS. 47.25F – Boundary layer and shear turbulence.

PACS. 61.30E – Experimental determinations of smectic, nematic, cholesteric, and lyotropic structures.

PACS. 64.70M – Transitions in liquid crystals.

**Abstract.** – Small-angle neutron scattering was employed to study the effect of shear flow on the nematic (N) and lamellar ( $L_x$ ) phases in aqueous solutions of cesium perfluoro-octanoate. Shear rates as high as  $\sim 4000 \text{ s}^{-1}$  were used. The N phase was found to align with the director in the direction of the gradient velocity. The  $L_x$  phase oriented with lamellae parallel to the shear plane. This change in equilibrium orientation is attributed, primarily, to changes in the value of the Ericksen viscosity parameter  $\alpha_2$ . Subtle shear-rate-dependent director reorientations were also observed in the proximity of the N-to- $L_x$  phase transition.

Shear is known to have a profound effect on the structure and macroscopic alignment of binary mixtures [1], diblock copolymers [2,3], colloidal suspensions [4], surfactant solutions [5], and monomer [6,7] and polymer [8] liquid crystals when the Deborah number,  $D = \dot{\gamma}\tau$ , approaches unity. Here,  $\dot{\gamma}$  is the shear rate and  $\tau$  is the characteristic time associated with molecular relaxations or fluctuations in a system. Typically, systems having short relaxation times require the use of large, sometimes unattainable, shear rates to induce detectable flow-dependent deformations. Because of this limitation, shear studies were first performed [4] on large-particle systems such as charged colloids. Large particles, having slower relaxation times, can be affected by much smaller shear rates. de Gennes [9] and Onuki [1] were among the first to point out that considerable effects could be seen at moderate shear rates on systems near a continuous phase transition. In such systems, the lifetime of a phase fluctuation diverges along with the correlation length as the transition is approached and, consequently,  $D$  approaches the value of one.

A number of different theoretical and experimental studies have been conducted to understand the effect of shear flow on phase transitions. Cates and Milner [10] have theoretically considered the Isotropic (I)-Lamellar ( $L_x$ ) phase transition and found that shear reduced fluctuations in the I-phase which resulted in an increase of the transition temperature toward its mean-field value, suggesting that the  $L_x$ -phase could be induced in the I-phase. This result was experimentally verified [2] in recent work on the order-disorder transition of a diblock copolymer. The I-to-nematic (N) phase transition in a liquid-crystal system was studied by Olmsted and Goldbart [7] who predicted an increase in the transition temperature with increasing shear rate up to a nonequilibrium critical point. Bruinsma and Safinya [11] considered a Landau theory of the

N-to-smectic-A (A) phase transition under shear. By applying a fluctuation correction to the nematic hydrodynamic model of Ericksen, Leslie and Parodi (ELP) [12], they predicted and later verified [6] a change in director orientations due to the divergent Ericksen viscosity parameter  $\alpha_3$  for thermotropic liquid crystals (TLC) with rod-like molecules.

The situation in liquid crystals with disk-shaped molecules, *i.e.* thermotropic discotic or lyotropic liquid crystals (LLC) with oblate micelles, is different from the conventional TLC with rod-like molecules. Such systems have been a subject of several theoretical investigations [13, 14]. However, to date, there have been very few experimental studies [15] of these materials under shear flow. In this paper, we report the effects of a Couette shear field on the N and  $L_x$  phases of a lyotropic liquid crystal with discotic micelles.

In the presence of a shear field, there are three possible configurations for the nematic director,  $\mathbf{n}$ , defined in fig. 1 for disk-like particles along with their characteristic scattering patterns. With the shear velocity,  $\mathbf{v} = v\hat{x}$ , and the gradient velocity ( $\nabla\mathbf{v}$ ) in the  $\hat{y}$ -direction, the *a* configuration has  $\mathbf{n} \perp (\mathbf{v}, \nabla\mathbf{v})$ -plane (to be referred to as the *shear plane*). The *b* configuration has  $\mathbf{n} \parallel \mathbf{v}$ , while in the *c* configuration  $\mathbf{n} \parallel \nabla\mathbf{v}$ . Each configuration has an associated viscosity,  $\eta_i$  ( $i = a, b, c$ ) known as Miesowicz [16] viscosities. The configuration obtained in a shear experiment depends upon the net balance of torques acting on  $\mathbf{n}$ .

In the high-shear regime, where elastic torques can be neglected, the equation of motion in the N-phase involves only the viscous torque [11] on  $\mathbf{n}$ ,

$$\Gamma_v = -\mathbf{n} \times [\gamma_1 \delta\mathbf{n}/\delta t + \dot{\gamma}(\alpha_2 n_y, \alpha_3 n_x, 0)], \quad (1)$$

where  $\alpha_2$  and  $\alpha_3$  are the Ericksen viscosity parameters which are defined in terms of the

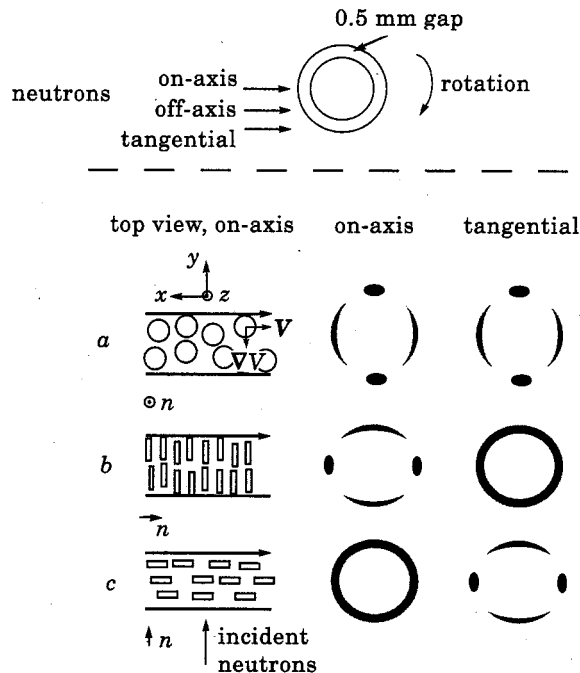


Fig. 1. - Top: top view of the shear cell, showing concentric cylinders and a gap filled by the sample. Arrows indicate the «on-axis», «tangential», and «off-axis» positions of the neutron beam. Bottom: three possible director configurations *a*, *b*, and *c* are shown under shear flow for discotic micelles along with their characteristic scattering pattern in the «on-axis» and «tangential» geometries.

rotational and shear viscosities,  $\gamma_1$  and  $\gamma_2$  as  $\alpha_2 = (\gamma_2 - \gamma_1)/2$  and  $\alpha_3 = (\gamma_2 + \gamma_1)/2$  with the restriction [12] that  $\alpha_3 > \alpha_2$ .

For a system of *rod-like* particles,  $\alpha_2$  is negative and the orientation of  $\mathbf{n}$  depends upon the sign of  $\alpha_3$ . In the N-phase, well above the N-A transition temperature,  $\alpha_3$  is also negative and the stable solution of the ELP equation requires that the director be oriented at a small (typically  $\sim 5^\circ$ ) angle  $\phi = \text{tg}^{-1} \sqrt{|\alpha_3/\alpha_2|}$  with respect to  $\mathbf{v}$ . As the A-phase is approached, an additional torque due to a flow-induced-fluctuation force renormalizes  $\alpha_3$  to give  $\alpha_3^R = \alpha_3 + (\pi/2)(k_B T/d^2)(\tau/\xi_{\parallel})$ , where  $d$  is the smectic periodicity and  $\xi_{\parallel}$  is the smectic correlation length parallel to  $\hat{\mathbf{n}}$ . Consequently,  $\alpha_3^R$  increases and becomes positive and the director reorients perpendicular to the shear plane, adopting the *a* configuration.

Lyotropic systems differ from thermotropics only in the shape and size of their microscopic entities. Since the dimensionality and symmetry of the lyotropic N and  $L_\alpha$  phases are the same as that of corresponding thermotropic phases, the same hydrodynamic equations can be used to describe them. The roles of the two viscosity coefficients are interchanged for discotic objects when compared to rod-like molecules. It has been shown that, in the nematic phase of discotic particles,  $\alpha_2$  and  $\alpha_3$  must be positive [13] and that  $\phi \sim 90^\circ$ . The director should orient parallel to  $\nabla \mathbf{v}$  and assume the *c* configuration. Although the angle  $\phi$  is quite different in the rod-like and discotic systems, the situation in the two cases is very similar. In both cases, the larger dimension of molecules or micelles (or the direction of smaller moment of inertia) lies parallel to  $\mathbf{v}$ . This should not be surprising as the steric forces are primarily responsible [14] for flow alignment. It has also been pointed out that in such systems  $\alpha_3$  is always positive but  $\alpha_2$  could change sign. When  $\alpha_2$  is positive, one obtains flow alignment with the director perpendicular to the shearing surfaces. On the other hand, if  $\alpha_2$  becomes negative, then no stable solution exists in the shear plane.

Solutions of CsPFO in water were studied by small-angle neutron scattering (SANS) to determine the effect of a shear field on the N and  $L_\alpha$  phases. We investigated a binary mixture of 55 wt% CsPFO in distilled, deionized, and degassed water (Isotropic 49.5 °C-N 44°C- $L_\alpha$ ). This system was chosen because of its simplicity and its isomorphism to TLC systems. In addition, the combination of CsPFO and water provided good scattering length contrast for neutron scattering experiments, eliminating the need to partially deuterate any components of the system.

The SANS study was carried out at the National Institute of Standards and Technology (NIST), Gaithersburg, at the 30 meter SANS spectrometer using neutrons of 5.0 and 5.5 Å wavelengths ( $\Delta\lambda/\lambda = 15\%$ ), pinhole collimation with sample aperture of 1.2 cm diameter, and sample-to-detector distance of 1.85 m. The Couette shear cell [17] used for this study (fig. 1) consisted of two concentric quartz cylinders with a 0.5 mm gap. Shear rates ranging from zero to 4000  $\text{s}^{-1}$  were used. Scattered neutrons were collected on a two-dimensional-area detector. Temperature was controlled by circulating water through an aluminum block inside the cell with temperature stability of  $\pm 0.5$  °C. The aluminum block had a skewed channel in it to allow the cell's center to be translated perpendicular to the neutron beam. This freedom enabled us to conduct scattering experiments in «on-axis», «off-axis», and «tangential» positions (fig. 1) permitting a three-dimensional determination of the director orientation. In the «on-axis» geometry the incident neutron beam points in the  $\nabla \mathbf{v}$  direction and momentum transfer vectors lie in the ( $y, z$ )-plane, *i.e.* the detector plane. In the «tangential» position, the neutron beam is parallel to  $\mathbf{v}$  and the detector plane contains  $\nabla \mathbf{v}$ -neutral directions. The «off-axis» position (with the cell displaced by half of its radius from the «on-axis» position) is a mixture of the other two cases. The data were corrected for background and empty-cell scattering, and analyzed by taking 20° sector averages parallel and perpendicular to the shear cell's axis of rotation which corresponded to the vertical and horizontal directions on the area detector, respectively.

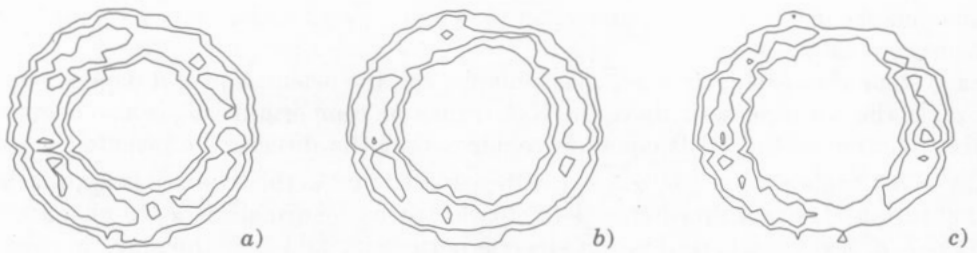


Fig. 2. – Contour plots of the data taken in the off-axis position in the N-phase at  $T = 49\text{ }^{\circ}\text{C}$  at shear rates of  $0.4$ ,  $4.0$ , and  $77.8\text{ s}^{-1}$  for the data shown in *a*), *b*), and *c*), respectively. Shear-rate-dependent anisotropy of the scattering ring shows improving director alignment in the horizontal ( $\nabla v$ -) direction as the system adopts the *c* configuration.

The data taken at  $49\text{ }^{\circ}\text{C}$  in the N-phase, fig. 2, shows the effect of increasing shear on the alignment of the N-phase in the off-axis configuration. The scattering ring became increasingly anisotropic with increasing  $\dot{\gamma}$  and eventually developed into two diffuse peaks at  $0.136\text{ \AA}^{-1}$  in the horizontal direction, such that the director  $\mathbf{n} \parallel \nabla v$  (*c* configuration). This inference is consistent with diffuse rings observed at slightly smaller  $q$  ( $= 0.129\text{ \AA}^{-1}$ ) in the on-axis geometry. This is in contrast to TLCs [13, 6] which assume the *b* configuration in the N-phase but in agreement with theoretical expectations. The reason for this difference is the dissimilarity of the particle shapes [13, 14] in the two systems, as discussed earlier.

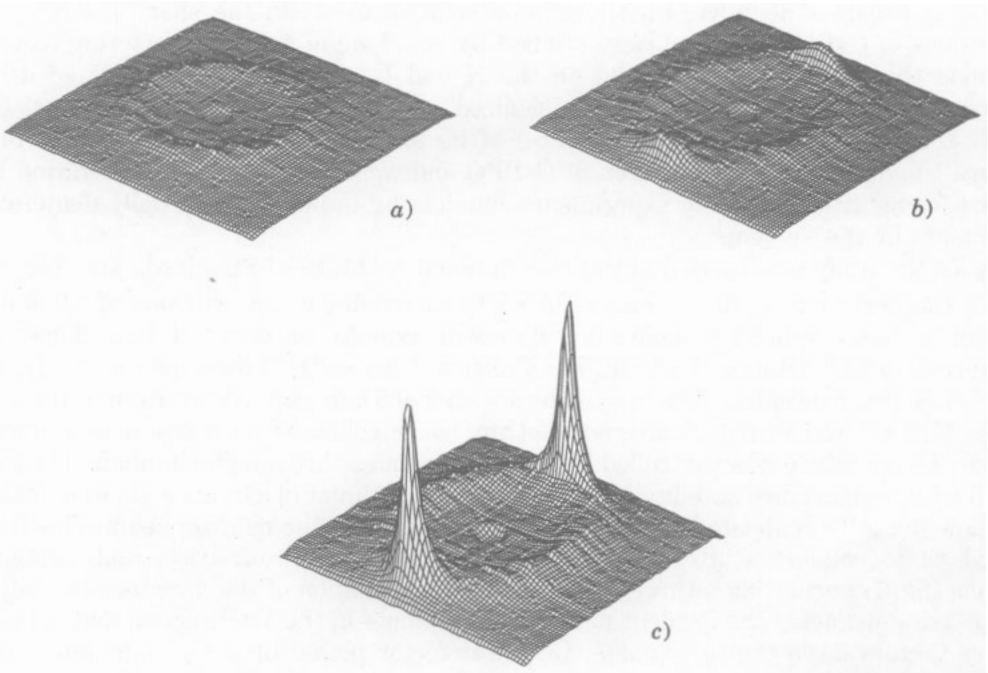


Fig. 3. – Scattering patterns in the  $L_{\alpha}$ -phase at  $42\text{ }^{\circ}\text{C}$  in the on-axis position at *a*)  $0.0$ , *b*)  $373.4$ , and *c*)  $933.6\text{ s}^{-1}$ . At zero shear,  $\mathbf{n}$  is randomly oriented. With increasing shear rate, a pair of sharp peaks develop in the vertical direction at  $q = \pm 0.146\text{ \AA}^{-1}$ , and two well-defined crescents appear in the *x*-direction at  $q = \pm 0.113\text{ \AA}^{-1}$ . This pattern indicates well-aligned lamellae in the *a* configuration, the crescents arise from intermicellar spacing within a lamella.

Figure 3 shows three-dimensional plots of the data collected in the on-axis configuration at different shear rates at 42 °C in the  $L_x$ -phase. At zero shear, the appearance of a broad diffuse circular ring indicated an unaligned sample. As the shear rate was increased, two rings corresponding to the two length scales of the system (diameter and thickness of the disks) began to emerge out of the diffuse ring. They had an uneven intensity distribution because of preferential alignment of the lamellae defined by the disk-like micelles, in essentially the same way as rod-like molecules define smectic-A planes. The outer ring developed into two sharp peaks in the vertical direction with increasing  $\dot{\gamma}$  while the inner ring took the form of two well-defined crescents in the (orthogonal) horizontal direction as a consequence of the director alignment perpendicular to the shear plane. Obviously, the system adopted the  $a$  configuration. This was consistent with the observations made when the cell was in the «off-axis» and tangential positions. This shear-induced alignment effect was found to be reversible, as a reduction in  $\dot{\gamma}$  was accompanied by a reduced degree of alignment. The sharp peaks at  $q = \pm 0.146 \text{ \AA}^{-1}$  were a result of well-aligned  $L_x$ -phase with layer spacing,  $d = 43 \text{ \AA}$ . The crescents, centered at  $q = \pm 0.113 \text{ \AA}^{-1}$ , were due to the intermicellar spacing of  $56 \text{ \AA}$  along their diameter within a lamella. The values of the intermicellar spacings obtained are in good agreement with independent X-ray measurements [18] for roughly the same concentration.

The effect of a change in temperature on the director's alignment was also probed at a constant shear rate of  $\dot{\gamma} = 97.3 \text{ s}^{-1}$  as the  $L_x$ -phase was approached from above. The results with the shear cell in the off-axis position are shown in fig. 4. At 49 °C, the appearance of crescents in the horizontal direction confirmed the  $c$  configuration as expected for the N-phase. Near  $T_{NL_x}$ , at 47 °C, the scattering pattern changed and the intensity in the vertical ( $z$ -) direction increased, suggesting that it was a mixture of the  $c$  and the  $a$  orientations. As the temperature was further lowered, the scattering patterns developed peaks in the vertical direction showing that the director assumed the  $a$  configuration at 44 °C in the  $L_x$ -phase. This behavior was indicative of a transition from the  $c$  to the  $a$  configuration as the system approached the N-to- $L_x$  phase transition. It suggested a change in the sign of  $\alpha_2$  due to renormalization. Unfortunately, this evident renormalization of  $\alpha_2$  has not been theoretically explored. It should be pointed out that the orientation of lamellae in this case is essentially identical to that of the smectic-A layers in TLCs and the  $L_x$ -phase [2, 6] of diblock copolymer melts.

Interesting shear-rate-dependent behavior was observed in close proximity of (0.5 to 1.5 °C higher than)  $T_{NL_x}$ . At low shear rates, the system was found to adopt the  $c$  configuration like the N-phase. But at higher shear rates it changed to the  $a$  configuration. For example, 1.5 °C above  $T_{NL_x}$ , configuration  $c$  was found to be stable up to  $\dot{\gamma} = 3.9 \text{ s}^{-1}$ . At higher  $\dot{\gamma}$ , the system was found to take up configuration  $a$ . At rates exceeding  $\sim 31 \text{ s}^{-1}$ , all alignment was lost.

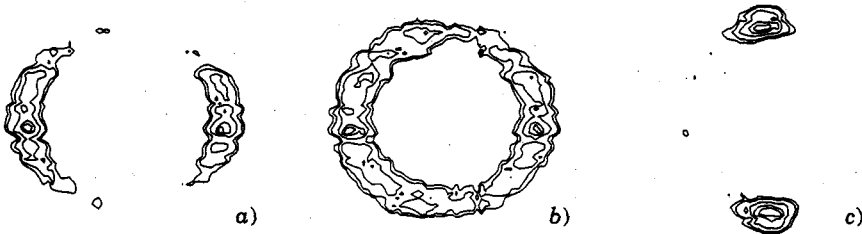


Fig. 4. - Contour plots with the shear cell in the off-axis position at a constant shear rate of  $97.3 \text{ s}^{-1}$  as the  $L_x$ -phase is approached from above. In the N-phase at 49 °C, the system aligns in the  $c$  orientation. As the temperature is lowered to 44 °C, the director undergoes a transition to the  $a$  orientation.

To summarize, we have studied the effect of a shear field on the lyotropic N and  $L_x$  phases. The  $L_x$ -phase aligned very well with increasing shear and little hysteresis was observed. The N-phase was found to adopt the  $c$  configuration while the  $a$  configuration was preferred in the  $L_x$ -phase. Our results suggest a renormalization of the viscosity parameter  $\alpha_2$  and a change in its sign from positive to negative as a consequence of divergent smectic correlations. These results should engender some theoretical interest and experimental investigations of the shear properties of discotic materials which, so far, appear to have been overlooked. It should also be interesting to study the shear properties of systems exhibiting uniaxial and biaxial nematic phases[19]. We plan to undertake SANS study on such materials.

\* \* \*

The authors wish to thank M. SRINIVASARAO and C. SAFINYA for helpful discussions. We are indebted to S. KEAST and M. E. NEUBERT for providing us with the high-purity CsPFO sample. Acknowledgement is made to the donors of The Petroleum Research Fund, administered by the ACS, for support of this research. The allocation of beam time on the NIST NG-3 30m SANS instrument is greatly appreciated. This material is based upon the activities supported by the National Science Foundation under Agreement No. DMR-91-22444. Identification of certain equipment and chemicals does not imply recommendation by the National Institute of Standards and Technology.

## REFERENCES

- [1] ONUKI A. and KAWASAKI K., *Ann. Phys. (N.Y.)*, **121** (1979) 456; BEYSENS D., GBADANASSI M. and BOYER L., *Phys. Rev. Lett.*, **43** (1979) 1253; HOBIE E. K., HAIR D. W., NAKATANI A. I. and HAN C. C., *Phys. Rev. Lett.*, **69** (1992) 1951.
- [2] KOPPI K. A., TIRRELL M. and BATES F. S., *Phys. Rev. Lett.*, **70** (1993) 1449; DIXON P. K., PINE D. J. and WU X. L., *Phys. Rev. Lett.*, **68** (1992) 2239.
- [3] BALSARA N. P. and HAMMOUDA B., *Phys. Rev. Lett.*, **72** (1994) 360.
- [4] CHEN L. B., ZUKOSKI C. F., ACKERSON B. J., HANLEY H. J. M., STRATY G. C., BARKER J. and GLINKA C. J., *Phys. Rev. Lett.*, **69** (1992) 688; CLARK N. A. and ACKERSON B. J., *Phys. Rev. Lett.*, **44** (1980) 1005; STEVENS M. J., ROBBINS M. O. and BELAK J. F., *Phys. Rev. Lett.*, **66** (1991) 3004.
- [5] KALUS J., HOFFMANN H., CHEN S. H. and LINDER O., *J. Phys. Chem.*, **93** (1989) 4267.
- [6] SAFINYA C. R., SIROTA E. B. and PLANO R. J., *Phys. Rev. Lett.*, **66** (1991) 1986; SAFINYA C. R., SIROTA E. B., BRUINSMA R. F., JEPPESEN C., PLANO R. J. and WENZEL L. J., *Science*, **261** (1993) 588.
- [7] OLMSTED P. D. and GOLDBART P., *Phys. Rev. A*, **46** (1992) 4966.
- [8] LARSON R. G. and MEAD D. W., *Liq. Cryst.*, **15** (1993) 151, and references therein.
- [9] DE GENNES P. G., *Mol. Cryst. Liq. Cryst.*, **34** (1976) 91.
- [10] CATES M. E. and MILNER S. T., *Phys. Rev. Lett.*, **62** (1989) 1856.
- [11] BRUINSMA R. and SAFINYA C. R., *Phys. Rev. A*, **43** (1991) 5377; BRUINSMA R. and RABIN Y., *Phys. Rev. A*, **45** (1992) 994.
- [12] ERICKSEN J. L., *Arch. Ration. Mech. Anal.*, **4** (1966) 231; LESLIE F. M., *Q. J. Mech. Appl. Math.*, **19** (1966) 357; PARODI O., *J. Phys. (Paris)*, **31** (1970) 581.
- [13] CARLSSON T., *J. Phys. (Paris)*, **44** (1983) 909; *Phys. Rev. A*, **34** (1986) 3393; *Mol. Cryst. Liq. Cryst.*, **89** (1982) 57; VOLVOVIK G. E., *JETP Lett.*, **31** (1980) 273.
- [14] HELFRICH W., *J. Chem. Phys.*, **50** (1969) 100; **53** (1970) 2267; FORSTER D., *Phys. Rev. Lett.*, **32** (1974) 1161.
- [15] KUZMA M., HUI Y. W. and LABES M. M., *Mol. Cryst. Liq. Cryst.*, **172** (1989) 211.
- [16] MIESOWICZ M., *Nature*, **158** (1946) 27.
- [17] STRATY G. C., *NIST J. Res.*, **95** (1989) 259.
- [18] CULL B., HEINO M., LEE S. H., KEAST S. S., NEUBERT M. E. and KUMAR S., *Liq. Cryst.*, **17** (1994) 507.
- [19] YU L. J. and SAUPE A., *Phys. Rev. Lett.*, **45** (1980) 1000.